Rethinking Statics: Enhancing Land Seismic Imaging with Full Waveform Inversion

Terence Krishnasamy, James Beck, Cristina Reta-Tang, Femi Ogunsuyi

Summary

This study presents a Full Waveform Inversion workflow to enhance velocity model accuracy in land seismic surveys. Unlike traditional approaches, no residual statics were applied, as FWI itself can incorporate these short-wavelength corrections in the derived velocity model. The effectiveness of this workflow is demonstrated through case studies in East Texas and the Delaware Basin. We also show that it is possible to capture shorter wave-length corrections in onshore data using FWI, which are normally addressed by residual statics.

Introduction

Near-surface characterization plays a crucial role in accurately imaging deeper targets, particularly in challenging onshore environments where low signal-to-noise ratios (SNR) and complex near-surface conditions can degrade data quality. Full Waveform Inversion (FWI) has emerged as a powerful tool to derive velocity models with high resolution and fidelity. Recently, though not as abundant as marine examples, we are seeing more successful application of FWI on land data examples (Plessix et al., 2012; Mei et al., 2015; Lemaistre et al., 2018; Tang et al., 2021; Masclet et al., 2021; Sheng et al, 2022; Krishnasamy et al., 2023, Gou et al., 2025).

In this study, we present an FWI workflow to enhance velocity model accuracy in land seismic surveys. We leverage both diving wave and reflection FWI (RFWI). We demonstrate the effectiveness of this workflow through case studies in East Texas and the Delaware Basin, showcasing improvements in imaging quality and show how we can reduce reliance on residual statics corrections.

Workflow

The initial near-surface model was built using diving wave tomography, supplemented where possible by shallow sonic logs. Pre-processing the data to make it suitable for full waveform inversion (FWI) is an important step. The focus of this step is to remove any unwanted energy that acoustic forward modeling is unable to capture, especially in the lower frequency ranges where the SNR is low. Key steps included high-amplitude noise suppression, ground-roll attenuation, and inverse Q corrections. Notably, no statics corrections were applied, as time-domain residual statics based on NMO velocities do not translate meaningfully to depth migration (Ellison & Innanen, 2016).

Due to the initial velocity model's uncertainty and limited low-frequency content, diving wave FWI without cycle skipping was initially unfeasible. To address this, we employed an optimal transport cost function using the quadratic Wasserstein distance (Engquist et al., 2016; Yang et al., 2018), which is less sensitive to the initial model accuracy. This facilitated robust low-wavenumber velocity updates.

With an improved background velocity model, we transitioned to dynamic matching FWI (DMFWI), which emphasizes kinematic differences over amplitude mismatches and mitigates noise using multi-channel windowing (Mao et al., 2020; Sheng et al., 2020). Refinement continued with reflection FWI (RFWI) using a pseudo-density model (Mao et al., 2019) to introduce density contrasts and generate synthetic reflection events. This approach reduced cycle skipping by leveraging near-angle time alignment and refining velocity updates through far-angle mismatches. The frequency bands used in RFWI were progressively increased.

Case Studies

The first dataset is from an onshore East Texas survey with 165 ft source and receiver spacing and 990 ft source line spacing. This survey was acquired with mixed source types, dynamite and Vibroseis, with a maximum offset of around 20,000 ft.

Diving wave FWI started at 5 Hz, employing a multi-scale approach where the frequencies were progressively increased. This multi-scale strategy helps to mitigate the risk of cycle-skipping by gradually introducing higher frequencies, allowing the inversion to converge more reliably. Figure 1 compares the results of running diving wave FWI up to 15 Hz. When comparing the velocity model from refraction tomography with that from FWI (figures 1c and 1d), we can see that the velocity model from FWI was able to capture very shallow velocity anomalies in the study area. The resulting PSDM image (Figure 1b), utilizing the velocity model from FWI, shows better event continuity and a more plausible geological structure. Surface-consistent mid- to long-wavelength statics and the corresponding surface consistent residual statics were recomputed using this model. Comparing the residual statics derived from long-wavelength statics using refraction tomography and the depth slice of the velocity model from FWI (Figures 2b and 2c), we observed a clear correlation between the anomalies identified by the FWI velocity model and higher residual

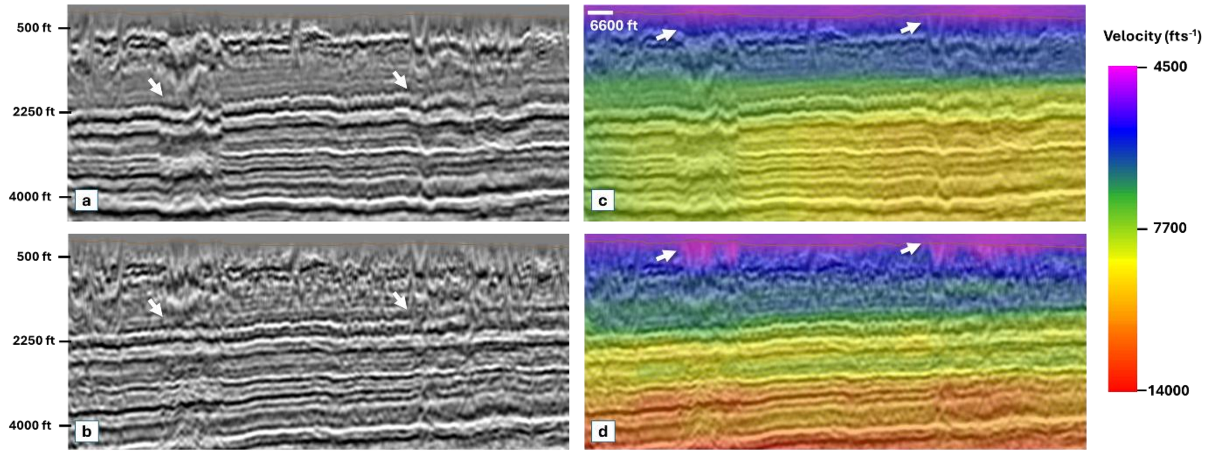

Figure 1, Diving wave FWI results from East Texas. a) Kirchhoff PSDM using initial velocity model b) Kirchhoff PSDM using the velocity model after diving wave FWI; c) Initial velocity model; d) Velocity model after diving wave FWI. The arrows show the distortion in the seismic image caused by shallow anomalies and improvement brought about by FWI.

statics values. This suggests that these anomalies would have been missed if residual statics were applied to our input data. Furthermore, we can clearly see a reduction in the residual statics post-FWI (Figure 2d), indicating that the FWI process was able to recover some of the mid- to short-wavelength corrections from the residual statics and transfer that to a velocity correction.

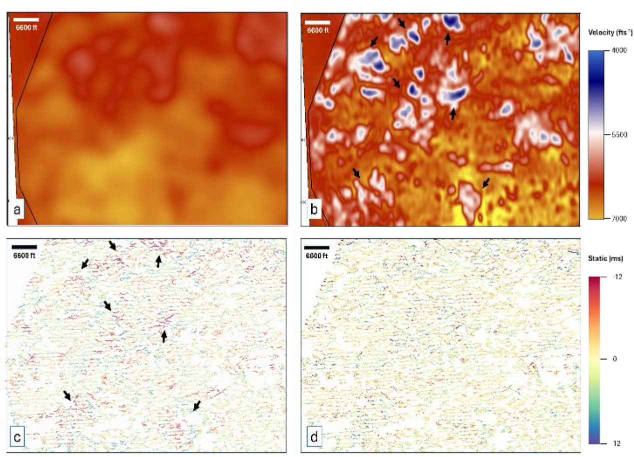

Figure 2: Depth slice at 500ft a) initial velocity model; b) velocity model after diving wave FWI; c) residual statics map, based on refraction tomography, d) residual statics map, based on the velocity model from diving wave FWI. The arrows highlight areas where there is a correlation between the velocity anomalies captured in the FWI velocity model and larger residual statics values.

The second dataset comes from the Delaware Basin, a challenging area due to Cenozoic fill. Historically, it has been difficult to image below this Cenozoic fill, where deeper events are distorted by the large shallow lateral velocity changes. The nominal shot and receiver spacing for the data acquired in this study is 165 ft, with source and receiver line spacing of 660 ft, with a maximum offset of around 23,000 ft. The survey used Vibroseis sources with a 2 Hz sweep, but the lowest usable frequency was about 5 Hz.

We started the diving wave FWI using the optimal transport cost function. This allowed us to compute more robust travel time information for the misfit calculation and avoid cycle skipping so that we could update the low wavenumber background velocity model where low frequencies were deficient. Following this, we transitioned to utilizing DMFWI to further refine the velocity model using the diving waves. A multi-scale approach was used in the DMFWI updates, and the frequencies were progressively increased to 12 Hz. Due to the limited penetration of diving waves into the shallow interbed halite and anhydrite layers, prevalent in the Delaware basin, an additional tomography step was necessary. Subsequently, the model updating was continued using RFWI. The frequencies used for RFWI were progressively increased to 15 Hz.

We show the resulting Kirchhoff PSDM sections and corresponding velocity model at different stages in the FWI velocity model building process (Figure 3). The line shown

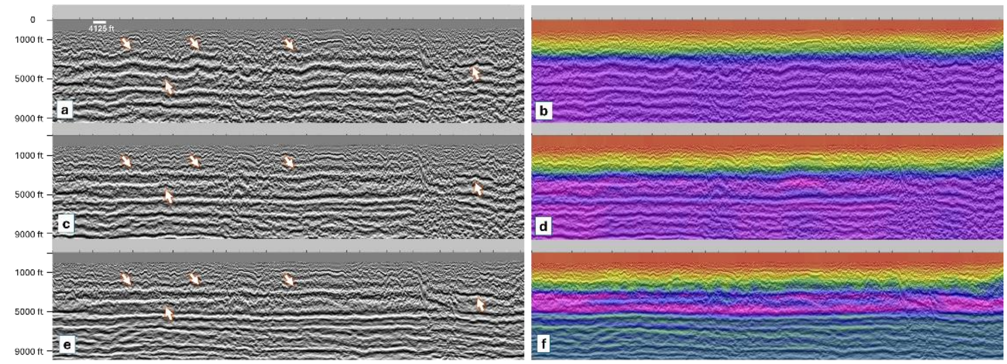

Figure 3: Kirchhoff PSDM and corresponding velocity model; a-b) after refraction tomography, initial model, c-d) after diving wave FWI, e-f) after reflection FWI. The arrows highlight areas where the seismic events show improvements after each stage of the velocity model updates using FWI.

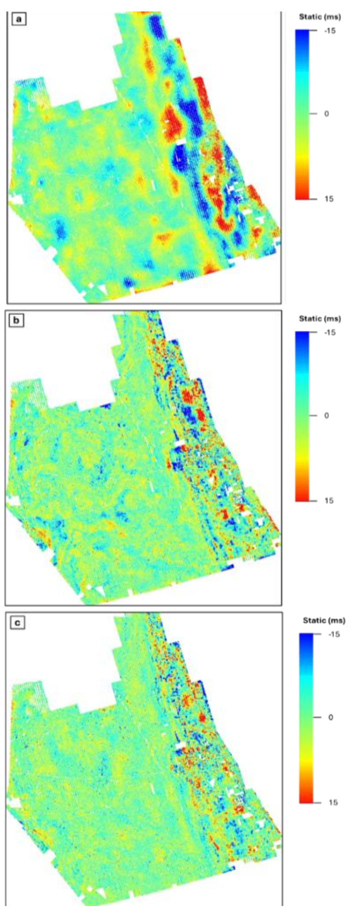

Figure 4: Surface consistent residual statics maps; a) computed after refraction tomography; b) computed after diving wave FWI; c) computed after reflection FWI.

cuts across the fill zone. We can see that FWI progressively corrects for the extreme lateral velocity changes in this area, addressing the undulation present on the deeper events and improving their coherence. Residual statics were computed at different stages of the FWI velocity model updates and are compared in Figure 4. These comparisons show a progressive reduction in mid- to short- wavelength statics present in the residual statics at each stage of FWI. This suggests that FWI recovered some of these static corrections and transferred them into a velocity correction at each stage

Conclusions

The utilization of FWI in these study areas presented several challenges that required careful consideration and strategic approaches. Our workflow was able to overcome these challenges, yielding velocity models that improve imaging quality. The successful application of our workflow to various onshore surveys, including challenging environments like the Delaware Basin, underscores its effectiveness.

We also show that it is possible to capture shorter wavelength corrections in onshore data using FWI, which are normally addressed by residual statics. This suggests that the approach of applying residual statics prior to FWI may not be the most effective strategy. Instead, allowing FWI to handle these corrections can lead to more accurate and detailed velocity models which might otherwise be obscured by the statics corrections.

Acknowledgments

We would like to thank TGS for permission to publish this work and our colleagues from the Land and Special Projects group for their help with data examples.

References

Ellison, D. and Innanen K., 2016, Improved resolution in depth imaging through reflection statics corrections derived from model-based moveout: CREWES Research Report, Vol 28, 2016.

Engquist, B., Froese, B.D. and Yang, Y., 2016, Optimal transport for seismic full waveform inversion: Communications in Mathematical Sciences, 14, 2309-2330.

Gou, Y., Aziz, A., Sedova, A., Renier, M., Donno, D., Lambare, G., Carotti, D., 2025, Unlocking onshore imaging challenges with FWI: Case studies from the sultanate of Oman, The Leading Edge, **44**, no. 1, 22–32.

Lemaistre, L., Brunellière, J., Studer, F. and Rivera, C., 2018, FWI on land seismic datasets with topography variations: Do we still need to pick first arrivals?: 88th Annual International Meeting, SEG, Expanded Abstracts, 1078–1082,

Krishnasamy, T., Sheng, J., Florendo, R., Beck, J., Sierra, A., Murphy, S., Siebens, J., Iwo-Brown, Y., 2023, High-resolution near surface velocity model building across the Delaware basin Fill zone using FWI: 84th Annual Conference and Exhibition, EAGE, Extended Abstracts.

Mao, J., Sheng, J. and Hilburn, G., 2019, Phase only reflection full-waveform inversion for high resolution model update: 89th Annual International Meeting, SEG, Expanded Abstracts, 1305–1309.

Mao J., Sheng, J., Huang, Y., Hao, F. and Liu, F., 2020, Multi-channel dynamic matching full-waveform inversion, 90th Annual International Meeting, SEG, Expanded Abstracts, 666-670.

Masclet, S., Bouquard, G., and Prigent, H., 2021, Multi-wave and full-waveform inversion in southern Oman: 82nd Conference and Exhibition, EAGE, Extended Abstracts.

Mei, J., Tong, Q., 2015 A practical acoustic full waveform inversion workflow applied to a 3D land dynamite survey: 85th Annual International Meeting, SEG, Expanded Abstracts, 1220-1224.

Plessix, R.É, G. Baeten, J.W. de Maag, F. ten Kroode, Z. Rujie, 2012, Full waveform inversion and distance separated simultaneous sweeping: a study with a land seismic data set. *Geophysical Prospecting*, **60**, 733-747.

Sheng, J., Mao, J., Liu, F., and Hart, M., 2020, A robust phase-only reflection full waveform inversion with multi-channel local correlation and dynamic minimum total-variation constraint: 82nd EAGE Conference & Exhibition, Extended Abstracts.

Sheng, J., Reta-Tang, C., Liu, F., Vázquez Cantú, A. and Cabrales Vargas, A., 2022, Full-waveform inversion and FWI imaging for land data, Second International Meeting for Applied Geoscience & Energy. August 2022, 827-831.

Tang, Y., Gaines, D., Hefti, J., Every, Z., Neumann, E., and Pharis, R., 2021, Land full-wavefield inversion for addressing complex near-surface challenges in the Delaware Basin: First International Meeting for Applied Geoscience and Energy, SEG/AAPG, Expanded Abstracts, 702-706.

Yang, Y., Engquist, B., Sun, J., and Hamfeldt, B., 2018, Application of optimal transport and the quadratic Wasserstein metric to full-waveform inversion: Geophysics **83(1)**, R43–R62.